

# Mixing of two-electron spin states in a semiconductor quantum dot

Ș. C. Bădescu and T. L. Reinecke

Naval Research Laboratory, Washington DC 20375

(Dated: November 3, 2018)

We show that the low lying spin states of two electrons in a semiconductor quantum dot can be strongly mixed by electron-electron asymmetric exchange. This mixing is generated by the coupling of electron spin to its orbital motion and to the relative orbital motion of the two electrons. The asymmetric exchange can be as large as 50% of the isotropic exchange, even for cylindrical quantum dots. The resulting spin mixing contributes to understanding spin dynamics in quantum dots, including light polarization reversal.

An electron spin in a semiconductor quantum dot (QD) is an attractive qubit for quantum computing [1]: the spin in the ground orbital state can have long coherence time [2]; a single qubit can be initialized or read optically by transient electron-hole pair excitation giving a negative trion  $X^-$  [3, 4]; and the manipulation of the spin exchange between neighboring spins can be the basis for two-qubit gates [1]. A detailed picture of correlations between spins in QDs is essential for understanding the spin dynamics. The dominant interaction between two electrons ( $e-e$ ) is the Heisenberg-like spin-symmetric  $J\hat{\mathbf{s}}_1 \cdot \hat{\mathbf{s}}_2$  (symmetric exchange), which conserves the total spin  $\hat{\mathbf{S}} = \hat{\mathbf{s}}_1 + \hat{\mathbf{s}}_2$ . Additional spin-asymmetric  $e-e$  interactions (asymmetric exchange) do not conserve  $\hat{\mathbf{S}}$  and thus decrease the fidelity of gate operations.

Among a number of recent experiments giving information about spin dynamics are those involving an optical polarization reversal [3, 4]. For them, it has been suggested that this effect results from spin flipping due to electron-hole ( $e-h$ ) exchange in QDs with lateral asymmetry. However, these experiments require strong spin mixing, inconsistent with  $e-h$  exchange alone [4].

Spin-orbit (s-o) interactions play a key role in understanding mixing of spin states. They arise from effective magnetic fields created by the orbital motion of electrons [5]. Electrons in QD ground states with dominant  $s$  components have small orbital angular momentum and thus small s-o coupling. A number of experiments of interest involve excited electrons in excited states of the QD. Linear combinations of nearly degenerate excited states in a plane (*e.g.*  $p_x$ - and  $p_y$ -like) can give rise to 2D orbital motion with an effective magnetic field perpendicular to the plane, and thus to large s-o coupling. This is analogous to the  $\hat{\mathbf{L}} \cdot \hat{\mathbf{S}}$  coupling in atoms [6]. Thus, relatively symmetric QDs (*e.g.* cylindrical) can have significant s-o effects, as we show here.

There are three sources of s-o coupling that lead to the mixing of spin states. The largest two contributions arise from the  $\mathbf{k} \cdot \hat{\mathbf{p}}$  mixing between the conduction and valence bands near the zone center, as described in the effective mass approach [7]. We derive them by treating the potentials from the structure and from the  $e-e$  Coulomb repulsion on the same footing with  $\mathbf{k} \cdot \hat{\mathbf{p}}$  terms, using the Kane model [8]. We have in mind QDs with a strong confinement to a single state  $\xi(z)$  along the growth axis  $\mathbf{e}_z$ ,

and a weaker confinement in the transverse directions, which give the electron states  $\phi_i(\mathbf{r}) = \xi(z)\varphi_i(\boldsymbol{\rho})$ .

The first contribution to the s-o coupling,  $\hat{\mathbf{h}}^V$ , arises from the *structure potential*  $V(\mathbf{r})$  of the QD. It gives a single-electron s-o coupling of the form [9]:

$$\hat{\mathbf{h}}^V \cdot \hat{\mathbf{s}} = \gamma_s^V [\partial_z V (\hat{\mathbf{p}}^\perp \times \hat{\mathbf{s}}^\perp) + (\partial_\rho V \times \hat{\mathbf{p}}^\perp) \hat{\mathbf{s}}^z] \mathbf{e}_z, \quad (1)$$

where  $p^z$  is not present due to the strong vertical confinement (for a single state  $\xi(z)$ ,  $\langle \xi | p^z | \xi \rangle = 0$ ). The first term in Eq.(1) is the usual Rashba coupling  $\gamma^V (\mathbf{e}_z \times \hat{\mathbf{p}}^\perp)$ , where  $\gamma^V = \gamma_s^V \langle \xi | \partial_z V | \xi \rangle$ , associated to asymmetry in the growth direction [10]. The second term is important for excited states whose main components are inversion-asymmetric ( $p$ -like), where it gives the dominant s-o coupling, independent of structure or bulk inversion asymmetries. This term vanishes in the QD ground state, whose main component is inversion-symmetric ( $s$ -like).

The second contribution,  $\hat{\mathbf{h}}^C$ , arises from the interaction of each spin with the orbital motion of the other. We have obtained it within a two-particle  $\mathbf{k} \cdot \hat{\mathbf{p}}$  approach for electrons interacting through the *Coulomb potential*  $U_C(\mathbf{r}_r)$  [11, 12]. For  $k=1, 2$  and  $\mathbf{r}_r = \mathbf{r}_1 - \mathbf{r}_2$ , we have:

$$\hat{\mathbf{h}}_k^C \cdot \hat{\mathbf{s}}_k = (-1)^k \gamma_s (\nabla_{\mathbf{r}_r} U_C \times \hat{\mathbf{p}}_k) \cdot \hat{\mathbf{s}}_k. \quad (2)$$

The coupling  $\hat{\mathbf{h}}^V$  from Eq.(1) is analogous to the Pauli s-o interaction, while  $\hat{\mathbf{h}}^C$  from Eq.(2) is analogous to the Breit-Pauli spin-relative orbit coupling [5]. The Pauli and Breit-Pauli couplings in vacuum or in atoms are relativistically small, due to the large energy gap  $2m_0c^2$  between electron and positron bands, whereas the present gap  $E_g$  is smaller, giving larger s-o couplings.

There is also a smaller contribution,  $\hat{\mathbf{h}}^B$ , from the *Dresselhaus coupling* due to the lack of bulk inversion symmetry [13]. It arises from the mixing of the conduction band with the remote upper bands and it gives a single-particle s-o coupling in the form  $\hat{\mathbf{h}}^B \cdot \hat{\mathbf{s}} = \gamma_b^B \epsilon^{\alpha\beta\delta} \hat{p}_\alpha (\hat{p}_\beta^2 - \hat{p}_\delta^2) \hat{s}_\alpha$ , with indices denoting crystal symmetry axis. In the QDs with strong vertical confinement consider here  $\langle p^{z2} \rangle \gg \langle p^{\perp 2} \rangle$ , thus the effective Dresselhaus coupling contains only the transverse components  $\mathbf{h}^{B,\perp} \simeq \gamma^B (\hat{p}_x, -\hat{p}_y)$ , with  $\gamma^B = \gamma_b^B \langle \xi | p_z^2 | \xi \rangle$ .

We use a model of QDs [14] resembling those from self-assembled growth [15] along crystal axis [001]. The lateral potential  $\mathcal{V}(\boldsymbol{\rho})$  contains a part  $\mathcal{V}_s$  symmetric for the

inversion  $\rho \rightarrow -\rho$ , and it may also contain an inversion-asymmetric part  $\mathcal{V}_a$  [16]. We take the principal axes  $e_{x,y}$  of the QD to be along the crystal axes [110] and  $[1\bar{1}0]$ . To construct accurate states we use a large basis set of harmonic oscillator wavefunctions. The lateral sizes  $a_x, a_y$  are given by the curvature at the potential minimum [17], which is determined entirely by the symmetric part  $\mathcal{V}_s$ .  $\mathcal{V}_a$  contains  $\mathcal{V}_{ax}$  ( $\mathcal{V}_{ay}$ ), odd in  $x$  ( $y$ ), and is parametrized by  $E_x$  ( $E_y$ ) [14]. The effective lateral electric field in the ground state  $\langle \varphi_1 | -\partial_{x,y} \mathcal{V}_a | \varphi_1 \rangle \propto E_{x,y}$  and vanishes for lateral inversion symmetry.

First we consider the two-electron wavefunctions without s-o coupling. They are obtained by diagonalizing hamiltonian  $H_0$  that contains the Coulomb interaction  $U_C = \frac{e^2}{\kappa r_r}$  ( $\kappa$  is the dielectric constant) with a band-mixing correction  $\gamma_c \delta(\mathbf{r}_r)$  [12] and the QD potential  $V(\mathbf{r})$ , in the basis of harmonic oscillator wavefunctions. These basis functions separate into the symmetric and antisymmetric sets  $\{S_n^{(0)}\}$ ,  $\{T_m^{(0)}\}$  by their permutation symmetry [18]. In general, each eigenstate of  $H_0$  can be written in terms of functions having definite  $s, x, y, d$  symmetry, *e.g.*:

$$\begin{aligned} T_1 &= T_1^x + E_x T_1^s + E_x E_y T_1^y + E_y T_1^d, \\ T_2 &= T_2^y + E_y T_2^s + E_x E_y T_2^x + E_x T_2^d, \\ S_2 &= S_2^x + E_x S_2^s + E_x E_y S_2^y + E_y S_2^d, \\ S_3 &= S_3^y + E_y S_3^s + E_x E_y S_3^x + E_x S_3^d, \end{aligned} \quad (3)$$

where  $T_1$  ( $T_2$ ) labels the lowest triplet with a larger  $x$  ( $y$ ) component, and  $S_2$  ( $S_3$ ) labels the lowest singlet with a larger  $x$  ( $y$ ) component. The lowest lying states are shown in Fig.1(a), where  $E_y=0$ . Higher lying states not shown are  $T_3$  ( $T_4$ ), which are the lowest  $d$  ( $s$ ) symmetry triplets, and  $S_4$  (the lowest  $d$ -symmetry singlet). The isotropic part of the exchange for a triplet  $T_i$  (with energy  $\epsilon_i^t$ ) and a singlet  $S_j$  (with energy  $\epsilon_j^s$ ) is given by  $J_{ij} = 2(\epsilon_i^t - \epsilon_j^s)/\hbar^2$ . Here we have chosen the energy splitting between the electron ground and excited states to be in the range 20–45 meV; this gives an exchange splitting ( $J_{13}$  between  $T_1$  and  $S_3$ ) of the order 5–10 meV, in the range of the experiments.

Next, the triplet-singlet mixing is generated by adding the s-o terms  $\mathbf{h}^V$ ,  $\mathbf{h}^C$ ,  $\mathbf{h}^B$  to  $H_0$ . These give a hamiltonian composed of a spin-symmetric part  $H_s$  that conserves the total spin, and a spin-antisymmetric part  $H_a$ :

$$H_s = H_0 + \frac{1}{2} \left( \hat{\mathbf{h}}_1 + \hat{\mathbf{h}}_2 + \gamma_s \partial_{\rho_r} U_C \times \hat{\mathbf{p}}_r^\perp \right) \cdot \hat{\mathbf{S}}, \quad (4)$$

$$H_a = \frac{1}{2} \left( \hat{\mathbf{h}}_1 - \hat{\mathbf{h}}_2 + 2\gamma_s \partial_{\rho_r} U_C \times \hat{\mathbf{p}}_c^\perp \right) \cdot (\hat{\mathbf{s}}_1 - \hat{\mathbf{s}}_2),$$

where  $\hat{\mathbf{h}}_k = \hat{\mathbf{h}}_k^V + \hat{\mathbf{h}}_k^B$ ,  $\hat{\mathbf{p}}_r = \hat{\mathbf{p}}_1 - \hat{\mathbf{p}}_2$ , and  $\hat{\mathbf{p}}_c = (\hat{\mathbf{p}}_1 + \hat{\mathbf{p}}_2)/2$ .  $H_a$  can be written as:

$$H_a = \sum_{i,j} \beta_{ij} \cdot (\hat{\mathbf{s}}_1 - \hat{\mathbf{s}}_2) |T_i\rangle \langle S_j| + h.c., \quad (5)$$

$$\beta_{ij} = \langle T_i | \hat{\mathbf{h}}_1 + \gamma_s \partial_{\rho_r} U_C \times \hat{\mathbf{p}}_c^\perp | S_j \rangle,$$

where  $\beta_{ij}$  gives the asymmetric exchange. States of different total spin  $|S\rangle$  are coupled via the operator  $\hat{\mathbf{s}}_1 - \hat{\mathbf{s}}_2$ ,

which is equivalent to the Dzyaloshinskii-Morya form  $\frac{2i}{\hbar} (\hat{\mathbf{s}}_1 \times \hat{\mathbf{s}}_2)$  [19]. The asymmetric exchange can be written:

$$\beta \cdot (\hat{\mathbf{s}}_1 - \hat{\mathbf{s}}_2) = \beta^z (\hat{s}_1^z - \hat{s}_2^z) + \beta^\perp \cdot (\hat{\mathbf{s}}_1^\perp - \hat{\mathbf{s}}_2^\perp). \quad (6)$$

The longitudinal component  $\beta^z$  conserves the total spin projection  $S^z$ , *i.e.*, it mixes singlets with triplets that have  $S^z=0$  ("longitudinal mixing"). This is equivalent to a precession of the total spin around axis  $e_z$  ( $\Delta S^z=0$ ). The transverse components  $\beta^\perp$  mix states with different total-spin projection ( $|\Delta S^z| \neq 0$ ), equivalent with a total-spin precession around in-plane axis ("transverse mixing").

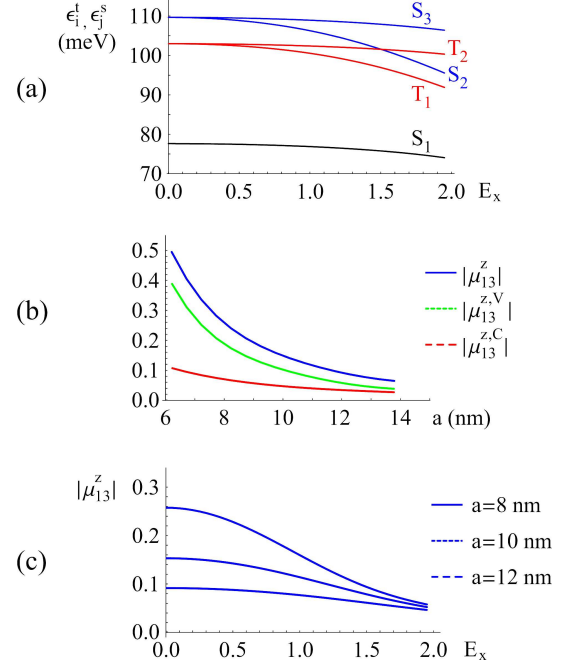


FIG. 1: (Color online) QDs with  $a_x=a_y=a$ . (a) Two-electron energy levels in QDs with  $a=10$  nm with one plane of symmetry along  $e_x$  ( $E_y=0$ ) vs the lateral asymmetry parameter  $E_x$ . (b) The asymmetric exchange  $|\mu_{13}^z|$  from Eq.(8) and its components  $|\mu_{13}^{z,V}|$  (from s-o coupling),  $|\mu_{13}^{z,C}|$  (from spin-relative orbit coupling) vs the QD size  $a$ . (c)  $|\mu_{13}^z|$  vs  $E_x \neq 0$  ( $E_y=0$ ) for several QDs.

It is convenient to group the operators from the matrix element giving  $\beta_{ij}$  in Eq.(5) into an axial vector operator  $\hat{\mathbf{A}} \equiv \hat{\mathbf{A}} e_z$  and two polar vector operators  $\hat{\mathbf{P}} \equiv \hat{\mathbf{P}} e_z$ ,  $\hat{\mathbf{R}} \equiv \hat{\mathbf{R}}^\perp$ :

$$\begin{aligned} \hat{\mathbf{A}} &= 2\gamma_s^V \left( \hat{\partial}_{\rho_1} \mathcal{V}_s \times \hat{\partial}_{\rho_1} \right) - 2\gamma_s \left( \partial_{\rho_r} U_C \times \hat{\partial}_{\rho_c} \right), \\ \hat{\mathbf{P}} &= 2\gamma_s^V \left( \hat{\partial}_{\rho_1} \mathcal{V}_a \times \hat{\partial}_{\rho_1} \right) \\ \hat{\mathbf{R}} &= -2\gamma^V \left( e_z \times \hat{\partial}_{\rho_1} \right) + 2\gamma^B \left( e_x \hat{\partial}_{x_1} - e_y \hat{\partial}_{y_1} \right). \end{aligned} \quad (7)$$

$\hat{\mathbf{A}}$  and  $\hat{\mathbf{P}}$  include the vertical magnetic field from the 2D motion in the nearly degenerate excited states, and they generate  $\beta^z$  in Eq.(6).  $\hat{\mathbf{R}}$  arises from the Rashba and Dresselhaus terms, and it generates  $\beta^\perp$ .

TABLE I: The part of the longitudinal coupling  $\beta_{ij}^z$  determined by  $\hat{A}$  [Eq.(7)]. The matrix elements  $A_{ij}^{\alpha\beta} = \langle T_i^\alpha | \hat{A} | S_j^\beta \rangle$  are between wavefunction components of definite symmetries [Eq.(3)].

	$S_1$ ( $\approx s$ -symmetry)	$S_2$ ( $\approx x$ -symmetry)	$S_3$ ( $\approx y$ -symmetry)	$S_4$ ( $\approx d$ -symmetry)
$T_4$ ( $\approx s$ )	$E_x E_y [A_{41}^{xy} + A_{41}^{yx} + A_{41}^{sd} + A_{41}^{ds}]$	$E_y [A_{42}^{sd} + A_{42}^{yx} + E_x^2 (A_{42}^{xy} + A_{42}^{ds})]$	$E_x [A_{43}^{sd} + A_{43}^{xy} + E_y^2 (A_{43}^{xy} + A_{43}^{ds})]$	$A_{44}^{sd} + E_x^2 A_{44}^{xy} + E_y^2 (A_{44}^{yx} + E_x^2 A_{44}^{ds})$
$T_1$ ( $\approx x$ )	$E_y [A_{11}^{xy} + A_{11}^{sd} + E_x^2 (A_{11}^{sd} + A_{11}^{yx})]$	$E_x E_y [A_{12}^{xy} + A_{12}^{yx} + A_{12}^{sd} + A_{12}^{ds}]$	$A_{13}^{xy} + E_y^2 A_{13}^{sd} + E_x^2 (A_{13}^{sd} + E_x^2 A_{13}^{yx})$	$E_x [A_{14}^{xy} + A_{14}^{sd} + E_y^2 (A_{14}^{sd} + A_{14}^{yx})]$
$T_2$ ( $\approx y$ )	$E_x [A_{21}^{yx} + A_{21}^{ds} + E_y^2 (A_{21}^{sd} + A_{21}^{xy})]$	$A_{22}^{yx} + E_x^2 A_{22}^{ds} + E_y^2 (A_{22}^{sd} + E_x^2 A_{22}^{xy})$	$E_x E_y [A_{23}^{xy} + A_{23}^{yx} + A_{23}^{sd} + A_{23}^{ds}]$	$E_y [A_{24}^{yx} + A_{24}^{ds} + E_x^2 (A_{24}^{ds} + A_{24}^{xy})]$
$T_3$ ( $\approx d$ )	$A_{31}^{ds} + E_x^2 A_{31}^{yx} + E_y^2 (A_{31}^{xy} + E_x^2 A_{31}^{sd})$	$E_x [A_{32}^{ds} + A_{32}^{yx} + E_y^2 (A_{32}^{xy} + A_{32}^{sd})]$	$E_y [A_{33}^{ds} + A_{33}^{yx} + E_x^2 (A_{33}^{xy} + A_{33}^{sd})]$	$E_x E_y [A_{34}^{xy} + A_{34}^{yx} + A_{34}^{sd} + A_{34}^{ds}]$

TABLE II: The part of the longitudinal coupling  $\beta_{ij}^z$  determined by  $\hat{P}$  [Eq.(7)].  $P_{ij}^{\alpha\beta} = \langle T_i^\alpha | \hat{P} | S_j^\beta \rangle$  are between wavefunction components of definite symmetry [Eq.(3)].

	$S_1$	$S_2$	$S_3$	$S_4$
$T_4$	$E_x [P_{41}^{sx} + P_{41}^{xs} + E_y^2 (P_{41}^{yd} + P_{41}^{dy})] + E_y [P_{41}^{sy} + P_{41}^{ys} + E_x^2 (P_{41}^{xd} + P_{41}^{dx})]$	$P_{42}^{sx} + E_x^2 P_{42}^{xs} + E_y^2 (P_{42}^{yd} + E_x^2 P_{42}^{dy}) + E_x E_y (P_{42}^{yx} + P_{42}^{xy} + P_{42}^{sd} + P_{42}^{ds})$	$P_{43}^{sy} + E_x^2 P_{43}^{yx} + E_y^2 (P_{43}^{zy} + E_x^2 P_{43}^{dx}) + E_x E_y (P_{43}^{xz} + P_{43}^{xs} + P_{43}^{yd} + P_{43}^{dy})$	$E_x [P_{44}^{sy} + P_{44}^{xd} + E_y^2 (P_{44}^{ys} + P_{44}^{dx})] + E_y [P_{44}^{sx} + P_{44}^{yd} + E_x^2 (P_{44}^{xs} + P_{44}^{dy})]$
$T_1$	$P_{11}^{xs} + E_x^2 P_{11}^{sx} + E_y^2 (P_{11}^{yd} + E_x^2 P_{11}^{dy}) + E_x E_y (P_{11}^{yx} + P_{11}^{xy} + P_{11}^{sd} + P_{11}^{ds})$	$E_x [P_{12}^{xs} + P_{12}^{sx} + E_y^2 (P_{12}^{sy} + P_{12}^{ys})] + E_y [P_{12}^{xd} + P_{12}^{dx} + E_x^2 (P_{12}^{sy} + P_{12}^{ys})]$	$E_x [P_{13}^{dx} + P_{13}^{sy} + E_y^2 (P_{13}^{yd} + P_{13}^{dx})] + E_y [P_{13}^{xd} + P_{13}^{dx} + E_x^2 (P_{13}^{sy} + P_{13}^{dx})]$	$P_{14}^{xd} + E_x^2 P_{14}^{dy} + E_y^2 (P_{14}^{dx} + E_x^2 P_{14}^{ys}) + E_x E_y (P_{14}^{xs} + P_{14}^{yd} + P_{14}^{dx} + P_{14}^{dy})$
$T_2$	$P_{21}^{ys} + E_x^2 P_{21}^{dx} + E_y^2 (P_{21}^{sy} + E_x^2 P_{21}^{dx}) + E_x E_y (P_{21}^{yd} + P_{21}^{dx} + P_{21}^{xs} + P_{21}^{ys})$	$E_x [P_{22}^{ys} + P_{22}^{dx} + E_y^2 (P_{22}^{sy} + P_{22}^{dx})] + E_y [P_{22}^{yd} + P_{22}^{xs} + E_x^2 (P_{22}^{dy} + P_{22}^{xs})]$	$E_x [P_{23}^{dy} + P_{23}^{xs} + E_y^2 (P_{23}^{yx} + P_{23}^{xs})] + E_y [P_{23}^{yd} + P_{23}^{xs} + E_x^2 (P_{23}^{dx} + P_{23}^{xs})]$	$P_{24}^{yd} + E_x^2 P_{24}^{dy} + E_y^2 (P_{24}^{xs} + E_x^2 P_{24}^{xs}) + E_x E_y (P_{24}^{yx} + P_{24}^{dx} + P_{24}^{ys} + P_{24}^{dx})$
$T_3$	$E_x [P_{31}^{dx} + P_{31}^{ys} + E_y^2 (P_{31}^{xd} + P_{31}^{sy})] + E_y [P_{31}^{dy} + P_{31}^{xs} + E_x^2 (P_{31}^{yd} + P_{31}^{xs})]$	$P_{32}^{dx} + E_x^2 P_{32}^{ys} + E_y^2 (P_{32}^{xd} + E_x^2 P_{32}^{sy}) + E_x E_y (P_{32}^{yd} + P_{32}^{xs} + P_{32}^{dx} + P_{32}^{ys})$	$P_{33}^{dy} + E_x^2 P_{33}^{yd} + E_y^2 (P_{33}^{xs} + E_x^2 P_{33}^{xs}) + E_x E_y (P_{33}^{yx} + P_{33}^{ys} + P_{33}^{dx} + P_{33}^{ys})$	$E_x [P_{34}^{dy} + P_{34}^{yd} + E_y^2 (P_{34}^{xs} + P_{34}^{xs})] + E_y [P_{34}^{dx} + P_{34}^{dx} + E_x^2 (P_{34}^{ys} + P_{34}^{ys})]$

Table I gives the matrix elements between  $T_i$  ( $i=1, 4$ ), and  $S_j$  ( $j=1, 4$ ), from the spin mixing operator  $\hat{A}$  in Eq.(7). The states are characterized by the symmetry of their dominant wavefunction components, *e.g.*  $S_2 \approx x$ -symmetry. Table II gives corresponding results from  $P$ . The terms in small boxes in Table I are dominant and are independent of lateral asymmetries. All the other terms in Tables I and II are non-zero only for cases of lateral asymmetry. The central  $2 \times 2$  block highlighted is of interest for the dynamics of  $X^-$  in the "p" shell [3, 4].

The matrix elements in Tables I and II can be understood by writing the operators in the basis  $\{|T_m^{(0)}, S_n^{(0)}\}$ :  $\hat{A} + \hat{P} = \sum_{m,n} (A_{mn} + P_{mn}) e_z |T_m^{(0)}\rangle \langle S_n^{(0)}| + h.c.$ . The matrix elements  $A_{ij}^{\alpha\beta}$  and  $P_{ij}^{\alpha\beta}$  in the tables are sums of the matrix elements  $A_{mn}$  and  $P_{mn}$  with the same symmetry. From Eq.(7), it is seen that  $A_{mn}$  is nonzero only for  $|T_m^{(0)}\rangle \langle S_n^{(0)}|$  odd both in  $x$  and in  $y$ , thus  $\hat{A}$  can produce longitudinal mixing  $\beta_{ij}^z$  between two-electron eigenstates  $T_i$  and  $S_j$  if one of these contains a  $x$  ( $s$ )-symmetry component, and the other has a  $y$  ( $d$ )-symmetry part [Table I].  $P_{mn}$  is non-zero only for QD asymmetries ( $V_a \neq 0$ ) and for  $|T_m^{(0)}\rangle \langle S_n^{(0)}|$  odd either only in  $x$  or only in  $y$ . Thus,  $\hat{P}$  contributes to the longitudinal spin mixing  $\beta_{ij}^z$  between  $T_i$  and  $S_j$  if one of them has a  $s$  or  $d$  component and the other has a  $x$  or  $y$  component [Table II].  $\hat{R}$  can be written as  $\hat{R} = \sum_{m,n} \mathbf{R}_{mn}^\perp |T_m^{(0)}\rangle \langle S_n^{(0)}| + h.c.$  Results for the matrix elements of  $\mathbf{R}_{mn}^\perp$  are not given explicitly here. They require QD lateral asymmetry and are nonzero for

$|T_m^{(0)}\rangle \langle S_n^{(0)}|$  odd in one of  $x$  or  $y$ . They can give transverse spin mixing  $\beta_{ij}^\perp$  of states with different  $z$  spin projection. The degree of triplet-singlet mixing is given by the ratio of the asymmetric to the symmetric exchange:

$$\mu_{ij}^z = \hbar^{-1} \beta_{ij}^z / J_{ij}, \quad \mu_{ij}^\perp = \hbar^{-1} \beta_{ij}^\perp / J_{ij}. \quad (8)$$

We now consider QDs with different asymmetries and consider the longitudinal spin mixing  $\mu^z$  from them. This mixing does not have contributions from the Dresselhaus and Rashba couplings.

*i. QDs with lateral inversion symmetry.* For them  $E_x = E_y = 0$ . Examples are shown in Fig.1(b) and by the  $E_x = 0$  points in Figs.1(a,c) and Fig.2. In such QDs, the two-electron states  $T_i, S_j$  have well-defined symmetries. The spin-mixing is due only to  $\hat{A}$ , on the second diagonal (in small boxes) in Table I. "Pure" states of  $x$  ( $y$ )-symmetry such as  $T_1$  ( $T_2$ ) couple only to "pure" states of  $y$  ( $x$ )-symmetry such as  $S_3$  ( $S_2$ ). The first order longitudinal spin mixing of  $T_1$  ( $T_2$ ) is from  $S_3$  ( $S_2$ ), which is the closest in energy.  $T_3$  (the lowest  $d$ -symmetry triplet) couples by  $\hat{A}$  to  $s$ -symmetry singlets like  $S_1$ .  $T_4$  (the lowest  $s$ -symmetry triplet) couples by  $\hat{A}$  to  $d$ -symmetry singlets such as  $S_4$ .

From Fig.1(b) and Fig.2 (at  $E_x = 0$ ) we can see that the asymmetric exchange can be a substantial fraction of the symmetric exchange (up to  $\approx 50\%$ ). Fig.1(b) shows that the asymmetric exchange is smaller for larger QDs, which results from larger orbits giving smaller effective magnetic fields in the s-o coupling. In this case  $\beta_{22}^z = -\beta_{13}^z$

because of degeneracy. The orbital momentum  $\hat{L}_z$  eigenstates  $\frac{1}{\sqrt{2}}(S_2 \pm iS_3)$  are strongly coupled to  $\frac{1}{\sqrt{2}}(T_1 \pm iT_2)$  and obey  $\Delta L_z = 0$ . From Fig. 2 we see that the asymmetric exchange decreases as the degeneracy of the first two excited states is removed by different  $a_x$  and  $a_y$ . In this case  $L_z$  is not conserved. The stronger confinement along  $e_y$  ( $a_x > a_y$ ) leads to  $J_{13} > J_{22}$ , and thus to  $|\mu_{13}^z| < |\mu_{22}^z|$ .

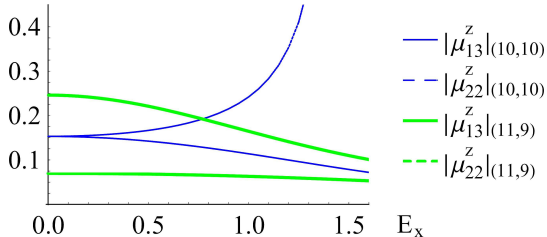


FIG. 2: (Color online) QDs with  $a_x \neq a_y$ . Asymmetric exchange  $\mu^z$  in QDs with  $a_x=11$  nm and  $a_y=9$  nm compared to the longitudinal coupling in QDs with  $a_x=a_y=10$  nm.

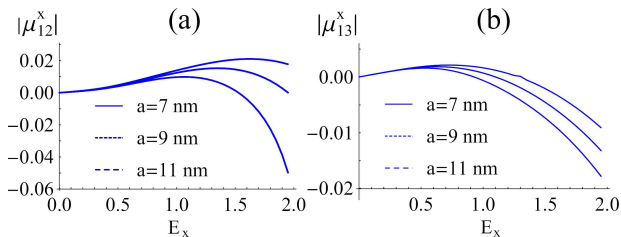


FIG. 3: (Color online) Mixing of states with different spin projection  $S^z$  in QDs with  $a_x=a_y$  and with a plane of symmetry ( $E_y=0$ ,  $E_x \neq 0$ ): (a)  $\mu_{12}^x$  for the mixing of  $T_1$  and  $S_2$ . (b)  $\mu_{13}^x$  for the mixing of  $T_1$  and  $S_3$ .

*ii. QDs with a single vertical plane of reflection.* For this case  $E_x \neq 0$  and  $E_y = 0$ . This gives more non-zero matrix elements in Tables I and II, *e.g.* now  $T_4$  is mixed with  $S_3$  as well as with  $S_4$ . This case is illustrated in Fig.1(a,c) and in Fig.2.  $\mu^z$  for the lowest triplet is seen to decrease with increasing  $E_x$ . For these cases, the terms proportional to  $E_x$  and  $E_x^2$  in Table I and also the terms from  $P=2\tilde{\gamma}^V(\partial_{\rho_1}\mathcal{V}_{ax} \times \hat{\partial}_{\rho_1})_{mn}^z \propto E_x$  from Table II are nonzero, and they tend to cancel partially the larger terms in the boxes in Table I. For some triplet-singlet pairs, such as  $S_3$  and  $T_1$ , the symmetric exchange becomes larger and thus their mixing decreases. Other singlet-triplet pairs can be degenerate, such as  $T_2$  and  $S_2$  in Fig.1(a) at  $E_x \approx 1.5$ ;

then nonzero  $\beta_{22}^z$  leads to strong singlet-triplet mixing [Fig.2]. For this case,  $L_z$  is not conserved. Triplets with  $\langle \hat{L}_z \rangle \approx \pm \hbar$  can be coupled to singlets that have  $\langle \hat{L}_z \rangle \approx \mp \hbar$ .

*iii. QDs with no vertical plane of reflection.* For this case  $E_x \neq 0$  and  $E_y \neq 0$ . Then all states in Tables I and II are mixed, and the degree of longitudinal spin mixing can be larger than in the previous cases.

In addition to the longitudinal spin-mixing described above, there is also mixing that changes the spin projection  $S^z$  (transverse mixing  $\mu^\perp$ ). This arises exclusively from the Dresselhaus and Rashba couplings, which give  $\mathbf{R}$  in Eq.(7). For QDs with lateral inversion symmetry,  $\mathbf{R}$  mixes states which typically differ by the single-particle energy splitting, *e.g.*  $T_1$  with  $S_1$  and  $S_4$  *etc.* For them the mixing from  $\mathbf{R}$  is small, due to large  $J_{11}$  and  $J_{14}$ . For QDs with only one vertical plane of reflection,  $\mathbf{R}$  mixes  $T_1$  with  $S_2$  or  $S_3$ , which are closer in energy and therefore give larger mixing. We show in Fig.3 this transverse spin-mixing for  $T_1$  and  $S_2$  and for  $T_1$  and  $S_3$ . This mixing occurs only for non-zero asymmetric potential ( $E_x \neq 0$ ). It is generally smaller than the longitudinal spin mixing discussed earlier, but it can become appreciable for large asymmetries, and it is larger in smaller QDs.

In recent experiments on light polarization reversal in QDs after excited state pumping [3, 4], the separation between excited  $p_x$  and  $p_y$ -like states is small and cannot be resolved. One picture of this effect [3, 4] is that it involves mixing of electron triplets and singlets with simultaneous spin flips of an electron and of the hole caused by axially-asymmetric  $e$ - $h$  exchange. For this mechanism, however, the experimental results require large QD asymmetries [4]. The additional mixing of triplets and singlets by asymmetric  $e$ - $e$  exchange here gives consistency with experiments using more realistic QD potentials.

In addition, the present results for triplet-singlet mixing provide an alternate process for the light polarization reversal. The angular momentum from the light can be given to the orbital motion of excited-state electrons. Then the triplet-singlet coupling given here can mix two-electron states that differ in their *orbital* angular momentum by  $2\hbar$ , leading to reversed light polarization. This is given for example in QDs with unequal lateral sizes even in the inversion-symmetric case (*i*) above.

We are grateful for discussions with Y. Lyanda-Geller, B. V. Shanabrook, D. Gammon and M. E. Ware. This work was supported in part by the ONR and by DARPA.

[1] D. Loss, D. P. DiVincenzo, Phys. Rev. A **57**, 120 (1998)  
 [2] M. Kroutvar *et al.*, Nature **432** (7013), 81 (2004)  
 [3] S. Cortez *et al.*, Phys. Rev. Lett. **89**(20), 207401 (2002)  
 [4] M. E. Ware *et al.*, Phys. Rev. Lett. **95**(17), 177403 (2005)  
 [5] V. B. Berestetskii, E. M. Lifshitz, L. P. Pitaevskii, *Quantum Electrodynamics*, (Butterworth-Heinemann, 1998)  
 [6] L. D. Landau and E. M. Lifshitz, *Quantum Mechanics*,

(Butterworth-Heinemann, 1998)

[7] G. L. Bir and G. E. Pikus, *Symmetry and Strain-induced Effects in Semiconductors*, (John Wiley & Sons, 1974)  
 [8] The Kane model [7] uses parameters: band gap  $E_g$ , energy of the split-off band  $\Delta$ , and matrix element  $P$  of operator  $\hbar\hat{p}_x/m_0$  between the Bloch states of the conduction and valence bands.

- [9]  $\gamma_s^V$  comes from the combination of the  $\mathbf{k}\cdot\hat{\mathbf{p}}$  band mixing with the potential for holes  $V_h = -c_h V$  ( $0 < c_h < 1$ ), which gives  $\gamma_s^V = -\frac{c_h}{\hbar^2} \frac{2P^2}{3E_g^2} \frac{\Delta(2E_g + \Delta)}{(E_g + \Delta)^2}$ . The procedure is the same as that for treatment of the Coulomb interaction [11, 12]
- [10] Yu. L. Bychkov, E. I. Rashba, JETP Lett. **39**, 78 (1984)
- [11] Ş. C. Bădescu *et al.*, Phys. Rev. B **72**, 161304(R) (2005)
- [12]  $\gamma_s$  comes from the combination of the  $\mathbf{k}\cdot\hat{\mathbf{p}}$  terms with the  $e$ - $e$  Coulomb potential, which gives  $\gamma_s = \frac{1}{\hbar^2} \frac{2P^2}{3E_g^2} \frac{\Delta(2E_g + \Delta)}{(E_g + \Delta)^2}$  [11]. This also gives to a spin-independent correction to the energy,  $\gamma_c \delta(\mathbf{r})$ , where  $\gamma_c = 2\pi \frac{e^2}{\epsilon} \frac{2P^2}{3E_g^2} \frac{(E_g + \Delta)^2 + E_g^2}{(E_g + \Delta)^2}$ .
- [13] G. Dresselhaus, Phys. Rev. **100**, 580 (1955).
- [14] We consider dots of height  $W$ , with confining potential  $V(\mathbf{r}) = -U_0 \theta(|z - W/2|)(1 + E_z z) \tilde{V}(\boldsymbol{\rho})$ , where  $U_0$  is the conduction band offset and  $\theta$  is the step function. The vertical function  $\xi(z)$  is the solution of  $V_z(z) = -U_0 \theta(|z - W/2|)(1 + E_z z)$ , and  $\varphi_i$  are solutions of the lateral potential  $\mathcal{V}(\boldsymbol{\rho}) = -U_0 \tilde{\mathcal{V}}(\boldsymbol{\rho})$ . For the symmetric part of the potential we use the Gaussian form  $\mathcal{V}_s(\boldsymbol{\rho}) = -U_0 e^{-(x/A_x)^2 - (y/A_y)^2}$ , and for the antisymmetric part we use  $\mathcal{V}_a(\boldsymbol{\rho}) = \mathcal{V}_s(\boldsymbol{\rho}) \left( E_x \left( \frac{x}{A_x} \right)^3 + E_y \left( \frac{y}{A_y} \right)^3 \right)$ .
- $E_{x,y}$  are perturbations to  $\mathcal{V}_s$  and characterize the lateral inversion asymmetry of the system. The energy scale of the lowest electron states is controlled by  $A_{x,y}$  and is chosen comparable to the experiment. Here we take  $W = 4$  nm and use InAs/GaAs parameters with a band offset  $U_0 = 0.6$  eV.
- [15] W. Seifert *et al.*, Prog. Cryst. Growth Ch. **33**, 423 (1996)
- [16] R. Krebs *et al.*, J. Cryst. Growth **251**, 742 (2003)
- [17] The single-particle basis is reducible to four subspaces:  $\{|s\rangle\}$  even in  $x$  and  $y$ ,  $\{|x\rangle\}$  odd in  $x$ ,  $\{|y\rangle\}$  odd in  $y$ , and  $\{|d\rangle\}$  odd in  $x$  and in  $y$ . If the system has inversion symmetry, these provide four independent subspaces for the eigenstates.
- [18] The two-particle basis is reducible to four subspaces, respectively of  $s$ ,  $x$ ,  $y$ , and  $d$ -symmetry. Symmetric combinations  $S_n^{(0)}$  form the singlet basis  $\{\sigma_{ss'}, \sigma_{xx'}, \sigma_{yy'}, \sigma_{dd'}\} \oplus \{\sigma_{sx}, \sigma_{yd}\} \oplus \{\sigma_{sy}, \sigma_{xd}\} \oplus \{\sigma_{xy}, \sigma_{sd}\}$ ; antisymmetric combinations  $T_m^{(0)}$  form the triplet basis  $\{\tau_{ss'}, \tau_{xx'}, \tau_{yy'}, \tau_{dd'}\} \oplus \{\tau_{sx}, \tau_{yd}\} \oplus \{\tau_{sy}, \tau_{xd}\} \oplus \{\tau_{xy}, \tau_{sd}\}$ .
- [19] I. E. Dzyaloshinskii, Phys. Chem. Solids **4**, 241 (1958); T. Morya, Phys. Rev. **120**, 91 (1960)